

A Zeolite-confined Pd/Acid Sites for High Efficiency of B–H Cleavage

Jia-Wen Liu,^[a, b] Si-Ming Wu,^{*,[a, c]} Yi-Tian Wang,^[b] Yuan Qin,^[b] Jing-Xian Wu,^[b] Li-Ying Wang,^{*,[d]} Ge Tian,^[b] Xiao-Fang Zhao,^[b] and Xiao-Yu Yang^{*,[b, c]}

Dedication with best wishes to Prof. Christoph Janiak on the Occasion of his 60th Birthday

Confining noble nanometal in zeolite framework is a promising way to improve its efficiency and durability for catalytic reactions. Herein, the synergistic effect of Pd nanoparticles and intrinsic acid sites in zeolite on promoting hydrogen generation performance is demonstrated. Pd nanoparticles are embedded into macroporous ZSM-5 (designed as Pd@ZSM-5) via a steam-thermal strategy. The confined Pd and acid sites in Pd@ZSM-5 synergistically promote the activation of ammonia borane (AB) and water molecules, resulting in the enhanced H₂ generation rates for AB hydrolysis. The interaction of Pd and acid sites in zeolite is further confirmed by solid-state NMR techniques and the key aspect is the confinement effect of zeolite. Furthermore, Pd@ZSM-5 shows high activity and durability in tandem hydrogenation of nitrobenzene.

The hydrolytic dehydrogenation of boron-based compounds with high hydrogen content, low molecular weight and good solubility is considered as an attractive way to generate hydrogen (H₂) for energy demand.^[1,2] Pd nanometal has been reported to be one of the most efficient catalyst for this H₂ evolution reactions, but the maximum utilization of active sites and high stability of nanoparticles is still needed for the practical application.^[3,4] Recently, various efficient supported Pd metal catalysts have been developed for the dehydrogenation of boron-based compounds for H₂ production.^[5,6] Zeolites, with prominent features of high surface area, good stability and highly ordered structure, are promising porous supports to Pd stabilization and cost decrease.^[7–9] In addition, the unique confinement effects of zeolite-confined Pd on a molecular scale enables spatially confined catalysis analogous to enzyme catalysis.^[10] The acid sites in solid acid catalyst has been reported to promote the dissociation and hydrolysis of boron-based compounds for enhanced H₂ production performance.^[11–13] Therefore, confining Pd nanometal in acidic zeolites can incorporate metals and acidic functions for the synergetic enhancement of the H₂ production. Moreover, the confined Pd nanometal can strongly affect the state of the acid sites while the zeolite framework can also influence the electronic structure and coordination state of Pd, thus possessing advantageous synergistic effects compared with the isolated Pd and acid sites.^[10,14–16]

Herein, macro-microporous ZSM-5 zeolite confined Pd nanoparticles (designed as Pd@ZSM-5) was synthesized by a direct steam-thermal crystallization approach. The synthesized Pd@ZSM-5 exhibits high H₂ generation rate from the hydrolytic dehydrogenation of ammonia borane (AB). Most significantly, it shows excellent activity and stability in the tandem dehydrogenation of boron-based compounds and reduction of nitro compounds. This work demonstrates a facile way for the rational design of zeolites-confined metal catalysts with high catalytic performance.

As shown in Scheme 1, Pd@ZSM-5 was prepared by steam-assisted crystallization of a dry gel with the molar composition of 1 SiO₂/0.01 Al₂O₃/0.12 TPAOH/0.0057 K₂PdCl₄ followed by calcination and H₂ reduction. (see ESI† for details).

As shown in SEM and TEM images (Figure 1a, b, Figure S1), zeolite particles have uniform size of about 2–3 μm with intracrystalline macropores (~500 nm). Powder X-ray diffraction

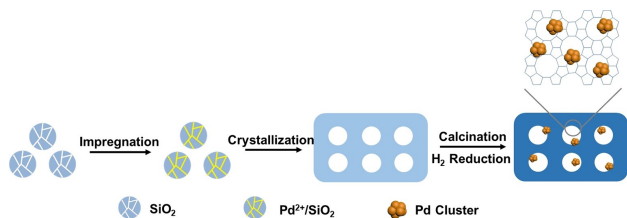
[a] J.-W. Liu, Dr. S.-M. Wu
School of Chemical Engineering and Technology & School of Materials, Sun Yat-sen University
Guangzhou, 510275, China
E-mail: simingwu6@syzu.edu.cn

[b] J.-W. Liu, Y.-T. Wang, Y. Qin, J.-X. Wu, Dr. G. Tian, X.-F. Zhao, Prof. X.-Y. Yang
State Key Laboratory of Advanced Technology for Materials Synthesis and Processing & School of Materials Science and Engineer & International School of Material science and Engineering, Wuhan University of Technology
122 Luoshi Road, Wuhan, 430070, China
E-mail: xyyang@whut.edu.cn

[c] Dr. S.-M. Wu, Prof. X.-Y. Yang
School of Engineering and Applied Sciences, Harvard University, Cambridge, MA 02138, USA
E-mail: simingwu@seas.harvard.edu
xyyang@seas.harvard.edu

[d] Dr. L.-Y. Wang
State Key Laboratory of Magnetic Resonance and Atomic and Molecular Physics
National Center for Magnetic Resonance in Wuhan
Wuhan Institute of Physics and Mathematics
Innovation Academy for Precision Measurement Science and Technology
Chinese Academy of Sciences, Wuhan, 430071
E-mail: lywang@wipm.ac.cn

Supporting information for this article is available on the WWW under <https://doi.org/10.1002/zaac.202000482>



Scheme 1. The schematic illustration of the fabrication of Pd@ZSM-5.

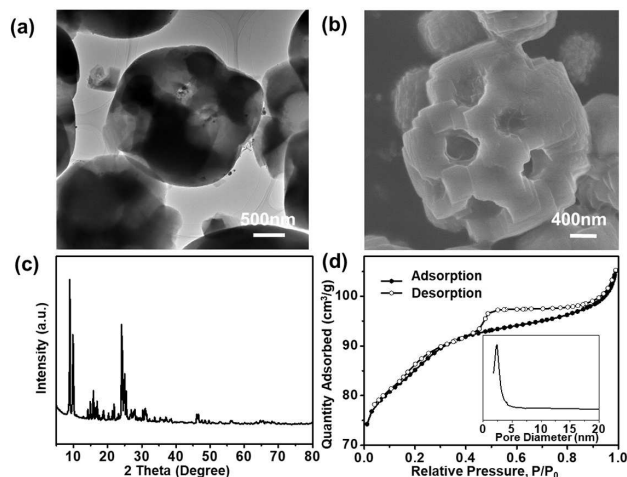


Figure 1. (a) TEM image and (b) SEM image of Pd@ZSM-5. (c) XRD pattern of Pd@ZSM-5. (d) N₂ adsorption/desorption isotherms and pore size distribution of Pd@ZSM-5.

pattern (Figure 1c) shows that Pd@ZSM-5 has a well-defined MFI structure without detectable peaks corresponding to Pd species, indicating the negligible lattice distortion after the encapsulation of Pd inside ZSM-5. N₂ adsorption isotherms and pore diameter distribution suggest that Pd@ZSM-5 has microporous and structure with additional mesopores. The structure and morphology of ZSM-5 (Figure S2, Table S1) has no significant difference from that of pure macroporous ZSM-5, indicating the introduction of Pd nanoparticles has no damage to the intrinsic structure of zeolite. Figure S3 shows the Pd 3d X-ray photoelectron spectroscopy (XPS) spectra of Pd@ZSM-5, which indicates that most the Pd precursor has been reduced to zero valence state.

The hydrolysis of AB as a typical hydrolytic hydrogenation reaction for H₂ generation is applied to investigate the catalytic performance of Pd@ZSM-5. And as comparison, Pd@S-1 (Silicalite-1 with MFI structure and no any acidic sites synthesized by our method), Pd/ZSM-5 (macroporous ZSM-5 supported Pd via impregnation), Pd/nano-ZSM-5 (nano-ZSM-5 supported Pd via impregnation) and commercial Pd/Al₂O₃ are also obtained. As measured by inductively coupled plasma atomic emission spectroscopy (ICP-AES) analysis (Table S2), all of the Pd-containing zeolites possess similar metal loadings of about 0.78 wt%. As shown in Figure 2a, Pd@ZSM-5 catalyst

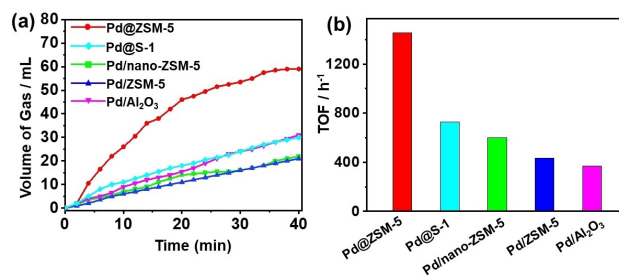


Figure 2. (a) Volume of the H₂ generated from AB hydrolysis versus time and (b) corresponding TOF values over different samples.

completed the hydrolysis of AB within 40 min, producing 60 mL H₂ ($n_{\text{Pd}}/n_{\text{AB}}=0.12$), affording a high turnover frequency (TOF) value of 1400 h⁻¹ (Figure 2b). Compared with the reported catalyst (Table S3), higher TOF values for ammonia borane hydrolysis is obtained in our work. This TOF value is about 2-fold of Pd@S-1, 2.4-fold of Pd/nano-ZSM-5, 3.4-fold of Pd/ZSM-5 and 3.9-fold of commercial Pd/Al₂O₃, respectively (Figure 2b, Table S2). Compared with Pd@S-1 using the same synthesis strategy, Pd@ZSM-5 has additional acid sites, which could be the main reason for its better catalytic performance. Therefore, it is important to gain insight into the acid sites with further investigations.

Solid-state nuclear magnetic resonance (NMR), which is capable of providing atomic-level information on intrinsic structure,^[17,18] has been widely used as an effective technique to probe the acid sites in zeolites.^[19–23] Pd@ZSM-5 is firstly characterized by one-dimensional (1D) ¹H solid-state magic angle spinning (MAS) NMR. As shown in Figure 3a, a strong signal at 3.7 ppm is observed in Pd@ZSM-5, which is assigned to the bridging hydroxyls species generated by Brønsted acid

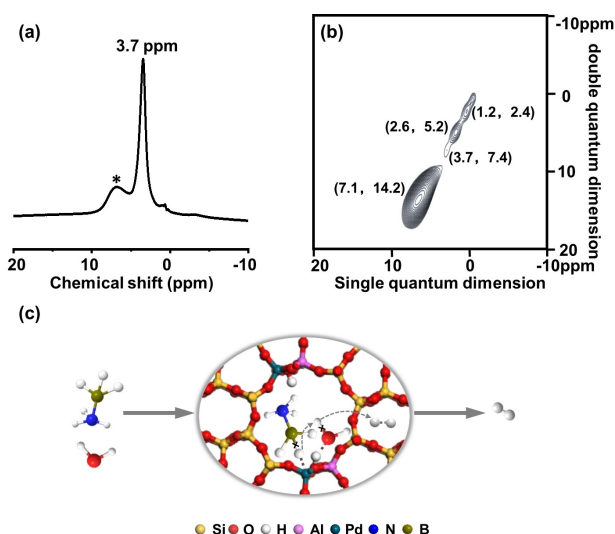


Figure 3. (a) ¹H solid-state MAS NMR spectra of Pd@ZSM-5. Asterisk represents the signal of rotor cap. (b) ¹H DQ-SQ MAS NMR spectra of Pd@ZSM-5. (c) Schematic illustration of proposed mechanism of AB hydrolysis over the model of Pd/acid sites.

sites (SiOHAl).^[13] The very weak signals in the range of 1–2 ppm belong to both terminal Si-OH protons and terminal hydroxyls arise from Lewis acid sites (AlOH).^[17] Two-dimensional (2D) ¹H-¹H double quantum (DQ)

MAS NMR, with the ability to provide the spatial proximity/interaction in the local structure,^[24–26] is further applied to gain deep insight into the interaction between acid sites of zeolite and Pd. The autocorrelation peaks at (1.2, 2.4) ppm, (2.6, 5.2) ppm and (3.7, 7.4) ppm in 2D ¹H DQ-SQ MAS NMR of Pd@ZSM-5 (Figure 3b) reveals the spatial proximity of terminal Si-OH protons, terminal Al-OH protons and Brønsted acid sites, respectively.^[22,27–30] A strong autocorrelation peak at (7.1, 14.2) ppm is attributed to the strong interaction between the trapped water molecules in the framework and Lewis acid sites.^[31] Notably, this signal indicates that Pd@ZSM-5 has strong adsorption ability of water molecules and enables the rapid exchange of the acidic protons with water. Therefore, the protonated water molecule activated by the acid sites can exert influence on AB hydrolysis along with Pd.

On the basis of catalytic results and characteristics, the possible mechanism of AB hydrolysis is shown in Figure 3c. In the reaction system, the confined Pd nanoparticles can firstly absorb AB molecules with further activation, resulting in the cleavage of B–H bonds.^[32–35] Meanwhile, the acid sites in zeolites can activate water molecules by transferring the proton from the acid sites to water.^[36,37] The dissociated H atoms from B–H bonds would bond with the protonated water molecule and lead to the formation of H₂ molecules. Therefore, the enhanced H₂ generation of Pd@ZSM-5 from AB hydrolysis could be attributed to the synergistic activation of AB and water molecules by the confined Pd/Acid sites. Another possible mechanism is that the promoted catalytic activity of AB hydrolysis is attributed to the change of electronic states of Pd caused by acid sites,^[38,39] although it will still need further characterizations.

To further verify the synergistic effect of Pd/acid sites, the tandem dehydrogenation of sodium borohydride and hydrogenation of nitrobenzene were also investigated. Pd@ZSM-5 shows the highest yield (98%) of aminobenzene in comparison with Pd@S-1 (78.7%), Pd/ZSM-5 (83.2%), Pd/nano-ZSM-5 (78.3%) and commercial Pd/Al₂O₃ (48%). It indicates that the increased hydrogen generation rates could promote the efficiency of tandem nitrobenzene hydrogenation. Besides, Pd@ZSM-5 also show over 80% of conversion rate after 5 cycles, indicating its good catalytic stability. The characterization of the recycled Pd@ZSM-5 after catalysis show a well-maintained crystal structure and morphology (Figure 4c), as well as the porous structure (Figure 4d). Therefore, confining Pd in ZSM-5 enables the successful stabilization of Pd nanoparticles and contribute to the synergy of Pd and acid sites in ZSM-5, thus resulting in the enhanced hydrogenation activity and good structural stability.

In summary, Pd nanoparticles have been successfully encapsulated in macroporous ZSM-5 zeolite by steam assisted crystallization method. The Pd@ZSM-5 shows high H₂ generation rates for AB hydrolysis owing to the interaction of Pd and the acid sites in zeolite, which is further investigated with solid-state NMR techniques. The mechanism of the synergistic activation of AB and

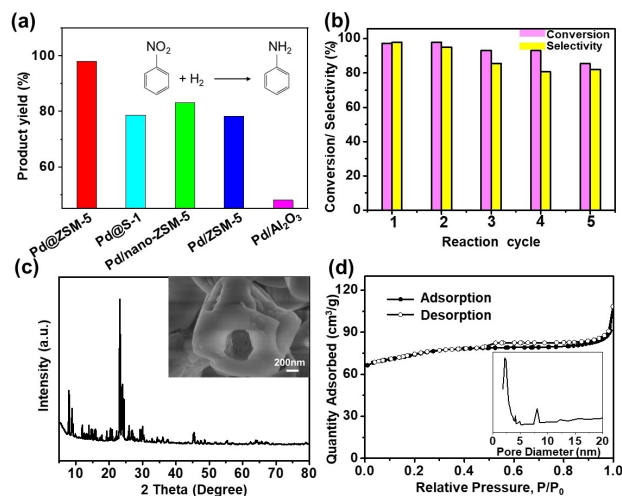


Figure 4. (a) Product yield of Pd@ZSM-5, Pd@S-1, Pd/nano-ZSM-5, Pd/ZSM-5, and Pd/Al₂O₃ in the reduction of nitrobenzene. (b) The performance of the recycled sample Pd@ZSM-5 in the reduction of nitrobenzene. (c) XRD pattern and SEM image (inset) of Pd@ZSM-5 after circulation. (d) N₂ adsorption/desorption isotherms and pore size distribution (inset) of Pd@ZSM-5 after circulation.

water molecules by Pd/Acid sites is proposed. Moreover, the zeolite-confined Pd catalyst exhibits high activity and stability in tandem hydrogenation of nitroarenes through coupling with dehydrogenation of boron-based compounds. This work not only provides a rational strategy for the design of zeolite-confined metal catalysts but also shows the great potential of such catalysts in tandem catalytic reactions.

Acknowledgements

X. Y. Yang acknowledges Prof. C. Janiak, as a mailstone and lighthouse, for his continuous help and scientific inspiration. This work was supported by a joint National Natural Science Foundation of China-Deutsche Forschungsgemeinschaft (NSFC-DFG) project (NSFC grant 51861135313), Sino-German Center COVID-19 Related Bilateral Collaborative Project (C-0046), Jilin Province Science and Technology Development Plan (20180101208JC), FRFCU (19lgzd16), ISTCP (2015DFE52870), Guangdong Basic and Applied Basic Research Foundation (2019A1515110435) and Guangdong Province International Scientific and Technological Cooperation Projects (2020A0505100036).

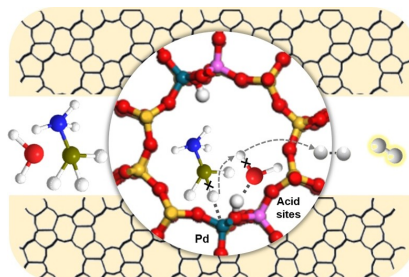
Keywords: Hierarchical nanostructure · confinement effect · specific catalysis · H₂ revolution · directed transformation

- [1] Q. Sun, N. Wang, Q. Xu, J. Yu, *Adv. Mater.* **2020**, *32*, 2001818.
[2] X.-L. Zhang, D.-X. Zhang, G.-G. Chang, X.-C. Ma, J. Wu, Y. Wang, H.-Z. Yu, G. Tian, J. Chen, X.-Y. Yang, *Ind. Eng. Chem. Res.* **2019**, *58*, 7209–7216.

- [3] Y.-X. Xiao, J. Ying, G. Tian, H. Wei, S.-Y. Fan, Z.-H. Sun, W.-J. Zou, J. Hu, G.-G. Chang, X.-Y. Yang, J. Christoph, *Appl. Catal. B* **2019**, *259*, 118080.
- [4] J. Wu, G.-G. Chang, Y.-Q. Peng, X.-C. Ma, S.-C. Ke, S.-M. Wu, Y.-X. Xiao, G. Tian, T. Xia, X.-Y. Yang, *Chem. Commun.* **2020**, *56*, 6297.
- [5] Z.-Y. Wen, Q. Fu, J. Wu, G.-Y. Fan, *Nanomaterials* **2020**, *10*, 1612.
- [6] M.-Y. Mao, Q. Chen, J. Wu, G.-Y. Fan, *Int. J. Hydrog. Energy* **2020**, *45*, 27244–27253.
- [7] X.-Y. Yang, L.-H. Chen, Y. Li, C. J. Rooke, C. Sanchez, B.-L. Su, *Chem. Soc. Rev.* **2017**, *46*, 481–558.
- [8] J. Zhang, L. Wang, B. Zhang, H. Zhao, U. Kolb, Y. Zhu, L. Liu, Y. Han, G. Wang, C. Wang, D. S. Su, B. C. Gates, F. S. Xiao, *Nat. Catal.* **2018**, *1*, 540–546.
- [9] T. L. Cui, W. Y. Ke, W. B. Zhang, H. H. Wang, X. H. Li, J. S. Chen, *Angew. Chem. Int. Ed.* **2016**, *55*, 9178–9182; *Angew. Chem.* **2016**, *128*, 9324–9328.
- [10] S.-M. Wu, X.-Y. Yang, J. Christoph, *Angew. Chem. Int. Ed.* **2019**, *58*, 12340–12354; *Angew. Chem.* **2019**, *131*, 12468–12482.
- [11] Q. Sun, N. Wang, R. Bai, Y. Hui, T. Zhang, D. A. Do, P. Zhang, L. Song, S. Miao, J. Yu, *Adv. Sci.* **2019**, *6*, 1802350.
- [12] R. Gil-San-Millan, A. Grau-Atienza, D. T. Johnson, S. Rico-Francés, E. Serrano, N. Linares, J. García-Martínez, *Int. J. Hydrog. Energy* **2018**, *43*, 17100–17111.
- [13] E. V. Grotthuss, S. E. Prey, M. Bolte, H. W. Lerner, M. Wagner, *J. Am. Chem. Soc.* **2019**, *141*, 6082–6091.
- [14] J.-W. Liu, S.-M. Wu, L.-Y. Wang, G. -Tian, Y. Qin, J.-X. Wu, X.-F. Zhao, Y.-X. Zhang, G.-G. Chang, L. Wu, Y.-X. Zhang, Z.-F. Li, C.-Y. Guo, C. Janiak, S. Lenaerts, X.-Y. Yang, *ChemCatChem* **2020**, *12*, 5364–5368.
- [15] S.-H. Li, A.-M. Zheng, Y.-C. Su, H.-L. Zhang, L. Chen, J. Yang, C.-H. Ye, F. Deng, *J. Am. Chem. Soc.* **2007**, *129*, 11161–11171.
- [16] Y.-C. Chai, S.-H. Liu, Z.-J. Zhao, J.-L. Gong, W.-L. Dai, G.-J. Wu, N.-J. Guan, L.-D. Li, *ACS Catal.* **2018**, *8*, 8578–8589.
- [17] J. Hu, Y. Lu, X.-L. Liu, J. Christoph, W. Geng, S.-M. Wu, Z.-X. Fang, L.-Y. Wang, G. Tian, Y. X. -Zhang, B.-L. Su, X.-Y. Yang, *CCS Chem.* **2020**, *2*, 1573–1581.
- [18] S.-S. Fan, L. Shen, Y. Dong, G. Tian, S.-M. Wu, G.-G. Chang, J. Christoph, P. Wei, J.-S. Wu, X.-Y. Yang, *J. Energy Chem.* DOI: 10.1016/j.jechem.2020.09.020.
- [19] M. Wang, N. R. Jaegers, M. Lee, C. Wan, J.-Z. Hu, H. Shi, D.-H. Mei, S. D. Burton, D. M. Camaioni, O. Y. Gutierrez, V. A. Glezakou, R. Rousseau, Y. Wang, J. A. Lercher, *J. Am. Chem. Soc.* **2019**, *141*, 3444–3455.
- [20] M. Dyballa, U. Obenaus, S. Lang, B. Gehring, Y. Traa, H. Koller, M. Hunger, *Microporous Mesoporous Mater.* **2015**, *212*, 110–116.
- [21] H. Huo, L.-M. Peng, C. P. Grey, *J. Phys. Chem. C* **2009**, *113*, 8211–8219.
- [22] P. Gao, Q. Wang, J. Xu, G.-D. Qi, C. Wang, X. Zhou, X.-L. Zhao, N.-D. Feng, X.-L. Liu, F. Deng, *ACS Catal.* **2018**, *8*, 69–74.
- [23] J. Xu, Q. Wang, F. Deng, *Acc. Chem. Res.* **2019**, *52*, 2179–2189.
- [24] Y. Lu, X.-L. Liu, L. He, Y.-X. Zhang, Z.-Y. Hu, G. Tian, X. Cheng, S.-M. Wu, Y.-Z. Li, X.-H. Yang, L.-Y. Wang, J.-W. Liu, J. Christoph, G.-G. Chang, W.-H. Li, T. V. Gustaaf, X.-Y. Yang, B.-L. Su, *Nano Lett.* **2020**, *20*, 3122–3129.
- [25] S.-T. Xiao, S.-M. Wu, Y. Dong, J.-W. Liu, L.-Y. Wang, L. Wu, Y.-X. Zhang, G. Tian, J. Christoph, S. Menny, Y.-T. Wang, Y.-Z. Li, R. K. Jia, B. W. Detlef, X.-Y. Yang, *Chem. Eng. J.* **2020**, *400*, 125909.
- [26] S.-M. Wu, X.-L. Liu, X.-L. Lian, G. Tian, C. Janiak, Y.-X. Zhang, Y. Lu, H.-Z. Yu, J. Hu, H. Wei, H. Zhao, G.-G. Chang, G. V. Tendeloo, L.-Y. Wang, X.-Y. Yang, B.-L. Su, *Adv. Mater.* **2018**, *30*, 1802173.
- [27] X.-F. Yi, K.-Y. Liu, W. Chen, J.-J. Li, S.-T. Xu, C.-B. Li, Y. Xiao, H.-C. Liu, X.-W. Guo, S.-B. Liu, A.-M. Zheng, *J. Am. Chem. Soc.* **2018**, *140*, 10764–10774.
- [28] I. Yarulina, K. D. Wispelaere, S. Bailleul, J. Goetze, M. Radersma, E. A. -Hamad, I. Vollmer, M. Goesten, B. Mezari, E. E. J. M. Hensen, J. S. MartinezEspin, M. Morten, S. Mitchell, J. Perez-Ramirez, U. Olsbye, B. M. Weckhuysen, V. Van Speybroeck, F. Kapteijn, J. Gascon, *Nat. Chem.* **2018**, *10*, 804–812.
- [29] S. Telalović, J. F. Ng, R. Maheswari, A. Ramanathan, G. K. Chuah, U. Hanefeld, *Chem. Commun.* **2008**, *38*, 4631–4633.
- [30] S.-H. Li, O. Lafon, W.-Y. Wang, Q. Wang, X.-X. Wang, Y. Li, J. Xu, F. Deng, *Adv. Mater.* **2020**, *32*, 2002879.
- [31] M. Hunger, D. Freude, H. Pfeifer, *J. Chem. Soc. Faraday Trans.* **1991**, *87*, 657–662.
- [32] S. Akbayrak, Z. Ozcifci, A. Tabak, *J. Colloid Interface Sci.* **2019**, *546*, 324–332.
- [33] K.-S. Yao, C.-C. Zhao, N. Wang, T.-J. Li, W.-W. Lu, J.-J. Wang, *Nanoscale* **2020**, *12*, 638–647.
- [34] Q.-L. Yao, K.-K. Yang, W.-D. Nie, Y.-X. Li, Z.-H. Li, *Renewable Energy* **2020**, *147*, 2024–2031.
- [35] S.-K. Kim, W.-S. Han, T.-J. Kim, T.-Y. Kim, S. W. Nam, M. Mitoraj, L. Piekos, A. Michalak, S.-J. Hwang, S. O. Kang, *J. Am. Chem. Soc.* **2010**, *132*, 9954–9955.
- [36] Q. Zhao, R. D. Dewhurst, H. Braunschweig, X. Chen, *Angew. Chem. Int. Ed.* **2019**, *58*, 3268–3278; *Angew. Chem.* **2019**, *131*, 3302–3313.
- [37] W. Chen, D. Li, Z. Wang, G. Qian, Z. Sui, X. Duan, X. Zhou, I. Yeboah, D. Chen, *AIChE J.* **2017**, *63*, 60–65.
- [38] Y. Lou, J. Ma, W. Hu, Q. Dai, L. Wang, W. Zhan, Y. Guo, X.-M. Cao, Y. Guo, P. Hu, G. Lu, *ACS Catal.* **2016**, *6*, 8127–8139.
- [39] W.-Y. Ke, T.-L. Cui, Q.-Y. Yu, M.-Y. Wang, L.-B. Lv, H.-H. Wang, Z.-D. Jiang, X.-H. Li, *Nano Res.* **2018**, *11*, 874–881.

Manuscript received: December 29, 2020
 Revised manuscript received: March 1, 2021
 Accepted manuscript online: March 7, 2021

SHORT COMMUNICATION



J.-W. Liu, Dr. S.-M. Wu, Y.-T. Wang, Y. Qin, J.-X. Wu, Dr. L.-Y. Wang*, Dr. G. Tian, X.-F. Zhao, Prof. X.-Y. Yang**

1 – 5

A Zeolite-confined Pd/Acid Sites for High Efficiency of B–H Cleavage

